# Joint Scalar PDF Simulations of a Bluff-Body Stabilised Flame with the REDIM Approach

B. Merci[*,1,2], B. Naud[3], D. Roekaerts[4] and U. Maas[5]

[1] Postdoctoral Fellow of the Fund of Scientific Research – Flanders (Belgium) (FWO-Vlaanderen)
[2] Ghent University – UGent, Dept. of Flow, Heat and Combustion Mechanics, Ghent, Belgium
[3]Modeling and Numerical Simulation Group, Energy Dept., Ciemat, Madrid, Spain
[4]Dept. of Multi-Scale Physics, Delft University of Technology, Delft, The Netherlands
[5]Institute for Technical Thermodynamics, Karlsruhe University (TH), Germany

**Abstract**

Transported joint scalar probability density function (PDF) results are presented for 'Sydney Flame HM3', a jet type turbulent flame with strong turbulence – chemistry interaction, stabilized behind a bluff body. We apply the novel Reaction-Diffusion Manifold (REDIM) technique, by which a detailed chemistry mechanism is reduced, including diffusion effects. Only $N_2$ and $CO_2$ mass fractions are used as reduced coordinates. A second-moment closure RANS turbulence model is applied. As micro-mixing model, the modified Curl's coalescence/dispersion (CD) and the Euclidean Minimum Spanning Tree (EMST) models are used. In physical space, agreement between experimental data and simulation results is good up to the neck zone, for the unconditional mean values of velocity, mixture fraction, major and some minor chemical species. Conditional mean profiles in mixture fraction space are also in reasonable agreement with experiments up to the neck zone, though conditional fluctuations tend to be under-predicted. CD generally yields better predictions for the level of fluctuations in mixture fraction space than EMST, but this is partly due to unrealistic particle evolution in composition space. In general, simulations using the REDIM approach for reduction of detailed $C_2$-chemistry confirm earlier findings for micro-mixing model behaviour, obtained with $C_1$-chemistry.

## Introduction

Turbulence-chemistry interaction is a central issue in non-premixed turbulent flame simulations. With the transported probability density function (PDF) technique, an exact treatment of the chemical reaction source term, given a certain chemistry model, is achieved [1]. Yet, reduction of chemistry is typically required in order to keep computing times within acceptable limits. In [2], where we present a comparative study on transported joint velocity-scalar PDF (JVSPDF) and joint scalar PDF (JSPDF) simulations, for the Sydney bluff-body stabilized flames 'HM1 and HM3' [3-6], we applied for the first time the novel Reaction-Diffusion Manifold (REDIM) technique [7] to reduce a detailed reaction mechanism, consisting of 34 species and 302 reactions [8]. This is a step forward, compared to the study of [9], where the influence of micro-mixing models was studied in the context of $C_1$-chemistry skeletal mechanisms. In [10] and [11], detailed and systematically reduced $C_2$-chemistry models are used, respectively. In [12], the conditional moment closure (CMC) is applied, with the GRI 2.11 or 3.0 chemistry mechanism.

In contrast to the study in [2], we focus here on the quality of the results in composition space for the JSPDF method. Previous studies [8-10] reveal that flame HM3, with the strongest turbulence – chemistry interaction effects of the series and which is close to blow-off conditions, is the most challenging flame.

In order to achieve good agreement to experimental data, up to the neck zone, for the turbulent flow field, a second moment closure model is applied with modified model constants [13]. Similarly, for good agreement in physical space for mean mixture fraction and mixture fraction variance, the turbulent Schmidt number is set to $Sc_T$ = 0.85 [2]. Two micro-mixing models are applied: the modified Curl's coalescence/dispersion (CD) [14] and the Euclidean Minimum Spanning Tree (EMST) model [15]. In [9], we showed that local extinction was underestimated with EMST and CD in general performed better, but no stationary solution could be obtained for HM3 with the CD mixing model. In the present study, applying reduced chemistry, obtained with the REDIM technique, a stationary solution is obtained, also with the CD mixing model.

## PDF Approach

All calculations are performed with the same hybrid Finite-Volume / particle methods, as implemented in the same in-house computer program 'PDFD' [16]. The statistical description of the flow is in terms of the joint one-point scalar PDF $f_\phi$: $f_\phi(\psi;x,t).d\psi$ is the probability that the composition vector $\phi$ is in the interval $[\psi,\psi+d\psi[$ at point $(x,t)$. The joint PDF is defined as [1,17]: $f_\phi(\psi;\mathbf{x},t)=\left\langle\delta\left[\phi(\mathbf{x},t)-\psi\right]\right\rangle$ . For variable density flows, it is useful to consider the joint scalar mass density function (MDF) $F_\phi(\psi)=\rho(\psi)f_\phi(\psi)$. Density weighted averages (Favre averages) can then be considered. Fluctuations with respect to the Favre average are defined as: $q''(\mathbf{x},t)=Q(\mathbf{x},t)-\tilde{Q}(\mathbf{x},t)$.The MDF transport equation is modelled and solved [1]:

Corresponding author: Bart.Merci@UGent.be

$$\frac{\partial F_\phi}{\partial t}+\frac{\partial \tilde{U}_j F_\phi}{\partial x_j}+\frac{\partial}{\partial \psi_\alpha}\left[S_\alpha(\boldsymbol{\psi})F_\phi\right]= -\frac{\partial}{\partial x_i}\left[\langle u_i''|\boldsymbol{\psi}\rangle F_\phi\right]-\frac{\partial}{\partial \psi_\alpha}\left[\langle \theta_\alpha|\boldsymbol{\psi}\rangle F_\phi\right] \quad (1)$$

with the mixing term $\theta_\alpha(\boldsymbol{\phi})=-\frac{1}{\rho(\boldsymbol{\phi})}\frac{\partial J_j^\alpha}{\partial x_j}$, and where $S_\alpha$ is the reaction source term for scalar $\phi_\alpha$ and $\boldsymbol{J}_\alpha$ its molecular flux. The first term on the right hand side is modeled using a gradient diffusion assumption: $\frac{\partial}{\partial x_i}\left[\langle u_i''|\boldsymbol{\psi}\rangle F_\phi\right]=-\frac{\partial}{\partial \mathrm{x_i}}\left[\Gamma_T\frac{\partial\left(F_\phi/\rho\right)}{\partial x_i}\right]$, where $\Gamma_T$ is the turbulent diffusivity, modeled as $\Gamma_T=\mu_T/\mathrm{Sc}_T$, with $\mu_T$ the eddy viscosity.

Mean velocity, mean pressure gradient, Reynolds stresses and turbulent dissipation rate are obtained by a standard Finite-Volume (FV) method based on a pressure-correction algorithm [2]. A particle method is applied for the solution of the MDF transport equation. A set of uniformly distributed computational particles evolves according to stochastic differential equations. Each particle has a set of properties $\{w^*, m^*, \boldsymbol{X}^*, \boldsymbol{\phi}^*\}$, where $w^*$ is a numerical weight, $m^*$ is the particle mass, $\boldsymbol{X}^*$ its position and $\boldsymbol{\phi}^*$ the particle's composition. Particle mass $m^*$ is constant in time. Increments of particle position $X^*$ and composition $\boldsymbol{\phi}^*$ over a small time step $dt$ are given by:

$$dX_i^*=\left[U_i^c\right]^* dt+\left[\tilde{U}_i+\frac{1}{\langle\rho\rangle}\frac{\partial\Gamma_T}{\partial x_i}\right]^* dt+\left[\left(\frac{2\Gamma_T}{\langle\rho\rangle}\right)^{1/2}\right]^* dW_i^*, \quad (2)$$

$$d\phi_\alpha^*=\theta_\alpha^* dt+S_\alpha\left(\boldsymbol{\phi}^*\right)dt. \quad (3)$$

The correction velocity $U_c$, resulting from a position correction algorithm [18], ensures that the volume represented by the particles in a computational cell, equals the cell geometric volume. In the random walk model for particle position evolution, $dW_i$ is an increments over $dt$ of the Wiener process $W_i$. All quantities between brackets [ ]* are FV properties interpolated at the particle location, using bilinear basis functions [19]. The method of fractional steps [1] is used to integrate the system of equations with local time-stepping [20]. More details on numerical issues are found in [2].

**Chemistry reduction by REDIM**

A recent comprehensive review on chemistry reduction is provided in [21,22], with arguments in favour of the 'close-parallel' assumption for chemistry based slow manifolds. We reduce the detailed reaction mechanism of [8], with 34 species and 302 reactions, by means of the REDIM technique [7], for a mixture of $CH_4/H_2$ and air as in HM3 (see below). This concept leads to an invariant low-dimensional manifold, directly accounting for the coupling of chemistry and diffusion (and convection). It is based on a relaxation process, where an initial guess for a low-dimensional manifold evolves in such a manner that an invariant slow reaction/diffusion manifold is obtained. This manifold, computed a priori, is steady and invariant in space in the turbulent flame simulations. One major advantage over ILDM, is the fact that a REDIM exists in the entire accessed domain, even at low temperatures (close to the unburned mixture), where chemistry is slow and ILDM does not yield an existing manifold. Close to equilibrium, the REDIM is close to ILDM. If chemistry governs the overall process, the REDIM concept yields slow manifolds or, equivalently, iteratively refined ILDMs as a limiting case [23].

In REDIM, an $m$-dimensional vector of reduced coordinates represents the composition vector $\boldsymbol{\phi}$. In order to simplify the subsequent use of the tables, suitable simple progress variables are identified after the calculation of the REDIM. They are used as the reduced coordinates. For the test case under study, we use $m = 2$ reduced coordinates: mixture fraction (or mass fraction of $N_2$) and mass fraction of $CO_2$ (the only reaction progress variable) [2]. Equal diffusivities and unity Lewis number are assumed in the present application of REDIM, although it is possible to extend the REDIM concept to systems with non-equal diffusivities. For the test cases under study, no evidence has been provided yet that differential diffusion would play an important role. In the transported PDF equations, it is also typically ignored in the micro-mixing modeling. In [2], we described some specific implementation details for the considered system.

In equation (1), the composition vector is thus reduced to $\boldsymbol{\phi} = (\xi, Y_{CO2})$ and the chemical source term $S_{CO2}(\boldsymbol{\phi})$ is given by the REDIM reduced chemistry. Note that in the experimental data below, the mixture fraction $\xi$ is defined on the basis of Bilger's formula [24]:

$$\xi=\frac{\frac{2(Z_C-Z_{C,o})}{W_C}+\frac{(Z_H-Z_{H,o})}{2W_H}-\frac{Z_O-Z_{O,o}}{W_O}}{\frac{2(Z_{C,f}-Z_{C,o})}{W_C}+\frac{(Z_{H,f}-Z_{H,o})}{2W_H}-\frac{Z_{O,f}-Z_{O,o}}{W_O}}. \quad (4)$$

where $Z_\beta$ is the total mass fraction of element $\beta$ and $W_\beta$ is its atomic mass. The subscripts "f" and "o" refer to the fuel and oxidant streams. In the present numerical results, where no differential diffusion is considered, mixture fraction is defined as: $\xi=1-\frac{Y_{N_2}}{Y_{N_2,o}}$.

**Micro-Mixing Modelling**

As mixing model $\theta_\alpha$, first the modified Curl's CD model [14] is used, which prescribes the evolution of particle composition as a series of pair-wise mixing events. The participating mixing particles are chosen at random from the set of particles present in a finite volume cell and their compositions change in the direction of the interaction partner. The degree of mixing in a pair is determined by a random variable, uniformly distributed between 0 (no mixing) and 1 (complete mixing). The model constant $C_\phi$ is set to 2.0, as in [2,9]. Comparison is also made to application of the EMST model [15], where particles interact preferably with neighboring particles in composition

space. As in [9], the model constant $C_\phi$ is then set to $C_\phi$ = 1.5, the default value for this mixing model. For comparison reasons, we also include results with $C_\phi$ = 2.0 with the EMST model.

**Test Case**

The gaseous fuel mixture of 50% $H_2$ and 50% $CH_4$ by volume, is injected from the central pipe, with diameter $D_j$ = 3.6mm, of the bluff-body burner, with outer diameter $D_b$ = 50mm. The burner is surrounded by an unconfined co-flow air stream. Fuel and air are mixed in the recirculation zone behind the bluff body where chemical reactions take place. The hot products stabilize the flame. In the experimental studies [3] and [4], the jet and co-flow bulk velocities were 214m/s and 40m/s (HM3). The velocity measurements, on the other hand, were provided for slightly reduced velocities (195m/s and 35m/s (HM3e)) [5]. The reader is referred to [6] for a more complete description.

The numerical settings are as described in [2]. A $6D_b$ long and $3D_b$ wide two-dimensional axisymmetric 160×128 structured grid is used, stretched in both axial and radial directions. Free-slip boundary conditions are prescribed on the bluff-body surface and on the lateral boundary. An average number of 100 particles per cell is used. Iteration averages are made over 500 iterations. As in [2], converged equilibrium chemistry assumed-shape β-PDF results are used as initial conditions. A statistically stationary situation is reached after about 5000 particle time steps. Results obtained after 20000 particle time steps are now discussed.

**Results in Physical Space**

We first illustrate the quality of the turbulent mixing fields. Due to space limitation, only two positions are considered: $x$ = 13mm, close to the burner; and $x$ = 90mm, which is in the 'neck zone' behind the recirculation region ($x > D_b$). For more results, including the turbulent flow field data, i.e. radial profiles of mean (axial) velocity and velocity fluctuations, we refer to [2], where good agreement to experimental data was illustrated, except for a well-known mean axial velocity under-prediction near the axis in the neck zone. We verified that there are practically no differences between CD and EMST results, confirming earlier findings reported in [9]. Figure 1 shows radial profiles of mean mixture fraction and mixture fraction variance. The profiles being slightly wide, agreement for mean mixture fraction is good. As expected, there is hardly any difference between the results, obtained with the different micro-mixing models. The mixture fraction variance is over-predicted near the burner. In the neck zone, agreement is quite good, although the profiles are again slightly too wide. The impact of the model constant $C_\phi$ is apparent: in the modeled mixture fraction variance transport equation, implied by the transported MDF equation [2], the scalar dissipation rate is lower with $C_\phi$ = 1.5, so that mixture fraction fluctuations are higher. Differences are small between the results, obtained with the two micro-mixing models, with the same $C_\phi$ value.

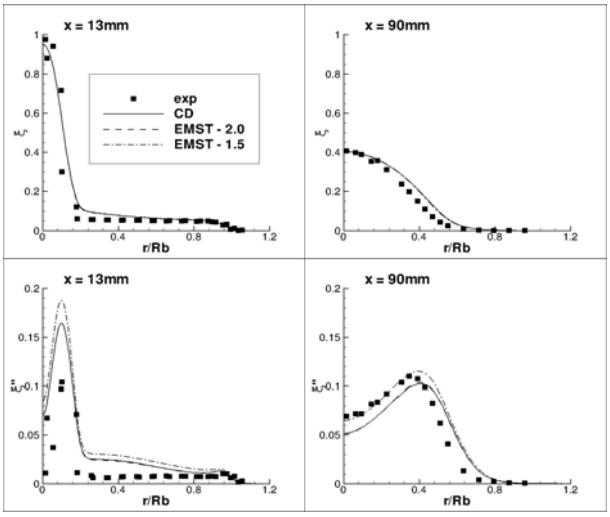


Figure 1. Radial profiles of mean mixture fraction and mixture fraction variance.

Figures 2 and 3 show radial profiles of mean temperature and some major and minor chemical species. The test case is challenging, as there is much local extinction (see below). Consequently, agreement with experimental data is not very good (and not as good as for HM1 [2], not shown here). One reason might be that the REDIM with only one reaction progress variable does not represent the thermo-chemical states well enough. This problem could be overcome by using a REDIM with two reaction progress variables. This remains to be investigated. Yet, the global shapes are well reproduced. It is instructive to observe that close to the burner ($x$ = 13mm), where there is relatively little local extinction, the simulation results are more affected by the choice of $C_\phi$ than by the choice of micro-mixing model, whereas in the neck zone this is less clear. This is also related to the discussion, reported in [9]: close to the burner, the micro-mixing time scale for the particles is relatively large, compared to mean convective and turbulent diffusion time scales. Consequently, the effect of the micro-mixing model is small in physical space results. In the neck zone, this is no longer true. Most interestingly, the arguments, provided in [9], with $C_1$ chemistry skeletal mechanisms, still hold with the present REDIM application with reduced $C_2$ chemistry.

**Results in Composition Space**

For the profiles of mean values and fluctuations, conditioned on mixture fraction, the mixture fraction interval [0,1] has been divided into 100 bins. For each bin, the arithmetic mean value and the fluctuations around these mean values have been computed accordingly, taking the root mean square value.

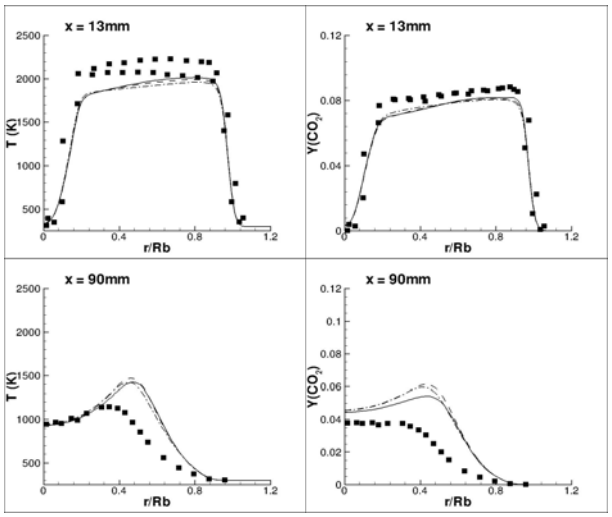


Figure 2. Radial profiles of mean temperature and $CO_2$ mass fraction.

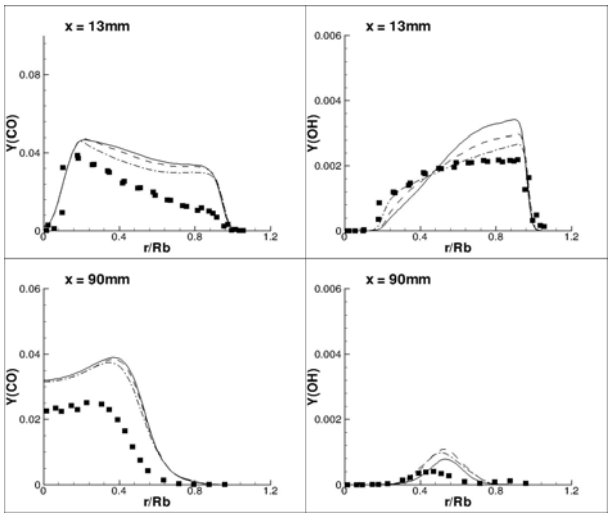


Figure 3. Radial profiles of mean *CO* and *OH* mass fraction.

Figure 4 shows conditional temperature profiles. At x = 13mm, agreement for the conditional mean temperature is quite good, but conditional fluctuations are under-estimated. Differences between the two micro-mixing models are small at x = 13mm, most probably because processes in physical space are more prominent than mixing/reaction in composition space [9]. At x = 90mm, differences between the micro-mixing models are apparent. While CD is closer to the experimental data, none of the results are in good agreement with experimental data: conditional mean temperatures are over-estimated and conditional fluctuations are under-predicted. As mentioned, probably the REDIM with only one reaction progress variable does not represent the thermo-chemical state well enough. This problem could be overcome by using a REDIM with two reaction progress variables.

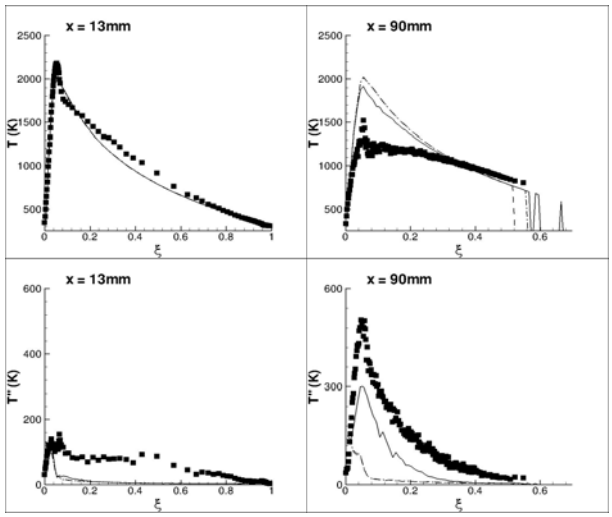


Figure 4. Profiles of conditional mean value and rms value of conditional fluctuations of temperature.

In figure 5, we present the profiles for major species and REDIM coordinate $CO_2$ mass fraction. There is a global over-prediction of conditional mean $CO_2$ mass fraction. The level of conditional fluctuations is in general under-predicted. It only seems correct with CD at $x$ = 90mm. Yet, note that the conditional mean values are still over-predicted.

Figure 6 shows minor species *OH*, which is particular in the sense that all the action takes place in the narrow region [0; 0.02] in mixture fraction space. In general, the experimental conditional mean values are over-predicted by a factor of two. Note the relatively small differences between CD and EMST, indicating that chemistry does not strongly intertwine with the micro-mixing modeling.

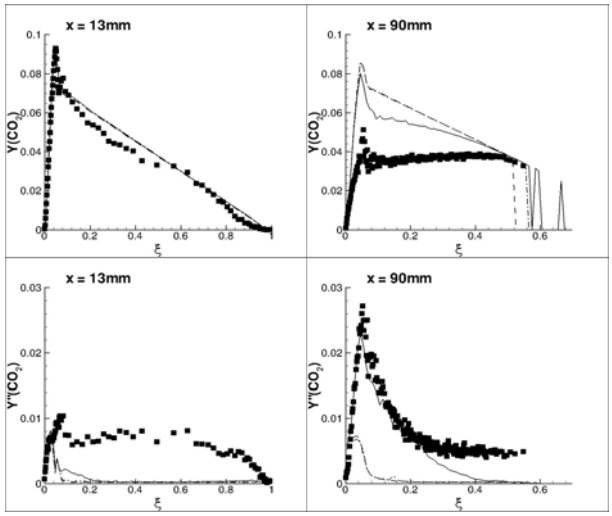


Figure 5. Profiles of conditional mean value and rms value of conditional fluctuations of mass fraction $CO_2$.

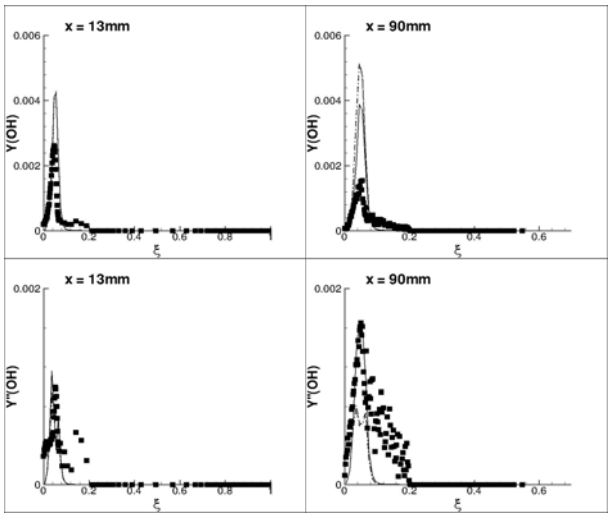

Figure 6. Profiles of conditional mean value and rms value of conditional fluctuations of mass fraction *OH*.

Figure 7, showing scatter plots of temperature versus mixture fraction, reveals strong differences between CD and EMST at $x$ = 90mm. With EMST, too little local extinction is seen. Again, it is interesting to note that these observations are completely in line with what was reported in [9], where we applied a $C_1$ chemistry based skeletal mechanism. Thus, chemistry does not seem to intertwine with these findings.

**Discussion**

In the present study, we applied the novel REDIM technique. Arguably, detailed comparisons to other techniques, such as the FPI/FGM (e.g. [25]), will be interesting future work. In particular, it will be interesting to investigate the importance of inclusion of diffusion effects in the construction of the manifold (as in REDIM) in limiting cases. This is considered beyond the scope of the present paper. Another issue is that the experimental data might not lie close to the REDIM manifold. This remains to be investigated.

**Conclusions**

The novel REDIM technique for reduction of a detailed chemistry model, has been applied to the turbulent non-premixed bluff body stabilized jet type flame HM3, which has strong turbulence – chemistry interaction and a substantial amount of local extinction.

Differences between results, obtained with two micro-mixing models on the one hand or with two different $C_\phi$ model constants on the other hand, have been explained. The interplay with phenomena in physical space has been highlighted.

The most important observation is that, in general, in composition space, earlier findings for micro-mixing model behavior, obtained with $C_1$ chemistry, have been confirmed with the REDIM approach for reduction of detailed $C_2$ chemistry.

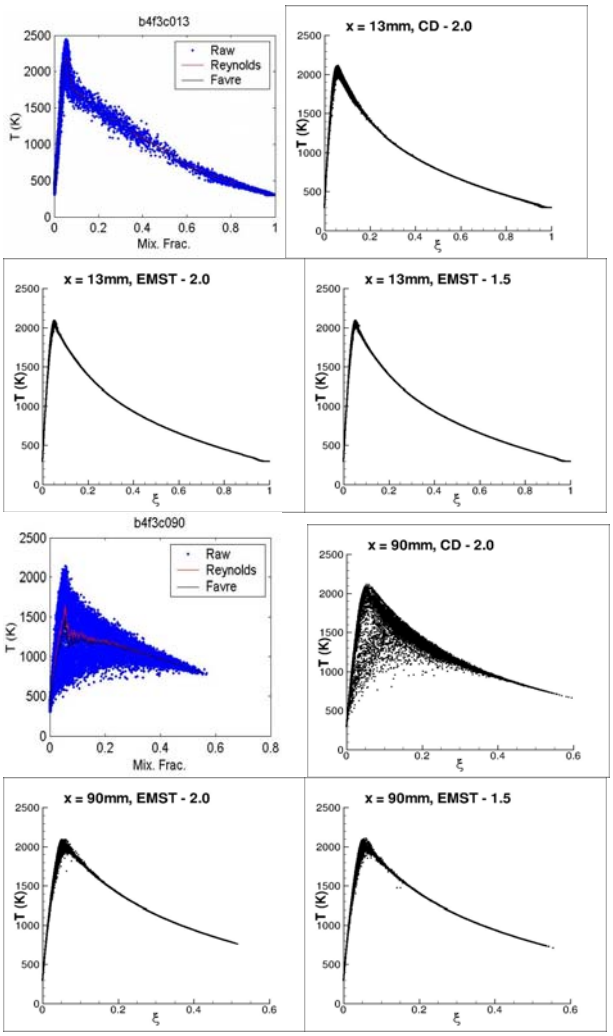

Figure 7. Scatter plots of temperature.

**Acknowledgements**

This collaborative research is supported by the COMLIMANS program, by the Spanish MEC under Project ENE 2005-09190-C04-04/CON and by the Fund of Scientific Research – Flanders (Belgium) (FWO-Vlaanderen) through FWO-project G.0079.07.

**References**

1. S.B. Pope. *Prog. En. Combust. Sci.*, 11:119-192, 1985.
2. B. Merci, B. Naud, D. Roekaerts and U. Maas, *Flow Turbul. Combust.* (in press). (DOI: 10.1007/s10494-008-9162-2)
3. B.B. Dally and A.R. Masri. *Combust. Theory Mod.*, 2:193-219, 1998.
4. B.B. Dally, A.R. Masri, R.S. Barlow, and G.J. Fiechtner. *Combust. Flame*, 114:119-148, 1998.
5. http://www.aeromech.usyd.edu.au/thermofluids/main_frame.htm
6. R.S. Barlow. International Workshop on Measurement and Computation of Turbulent Nonpremixed Flames. http://www.ca.sandia.gov/TNF
7. V. Bykov and U. Maas, *Combust. Theory Mod.* 11(6): 839-862, 2007.

8. J. Warnatz, U. Maas, R. W. Dibble: Combustion, Springer (1996). [ISBN:3-540-60730-7]
9. B. Merci, D. Roekaerts, B. Naud and S.B. Pope. *Combust. Flame* 146:109-130, 2006.
10. K. Gkagkas, R.P. Lindstedt and T.S. Kuan, *Flow, Turbulence and Combustion* (in press). (DOI: 10.1007/s10494-008-9164-0)
11. R.P. Lindstedt, H.C. Ozarovsky, R.S. Barlow and A.N. Karpetis, *Proc. Combust. Inst.* 31:1551-1558 (2007).
12. S. Sreedhara and K.Y. Huh, *Combust. Flame* 143 (1-2):119-134, 2005.
13. G. Li, B. Naud and D. Roekaerts. *Flow, Turbul. Combust.*, 70:211-240, 2003.
14. J. Janicka, W. Kolbe and W. Kollmann. *J. Non-Equil. Thermod.*, 4:47-66, 1979.
15. S. Subramaniam and S.B. Pope, *Combust. Flame* 115: 487-514, 1998.
16. B. Naud, C. Jiménez and D. Roekaerts. *Prog. Comp.l Fluid Dyn.*, 6:146-157, 2006.
17. S.B. Pope. *Turbulent Flows*, Cambridge University Press, 2000.
18. M. Muradoglu, S.B. Pope, and D.A. Caughey. *J.Comp. Phys.*, 172:841-878, 2001.
19. P. Jenny, S.B. Pope, M. Muradoglu, and D.A. Caughey. *J. Comp. Phys.*, 166:218-252, 2001.
20. M. Muradoglu and S.B. Pope. *AIAA J.*, 40:1755-1763, 2002.
21. Z. Ren and S.B. Pope, *Combust. Flame* 147: 243-261, 2006.
22. Z. Ren and S.B. Pope, *Combust. Theory Mod.* 11(5): 715-739, 2007.
23. J. Nafe and U. Maas, *Combust. Theory Mod.* 6: 697-709, 2002.
24. R.W. Bilger, S.H. Starner and R.J. Kee. *Combust. Flame*, 80:135-149, 1990.
25. L. Vervisch, R. Hauguel, P. Domingo and M. Rullaud, J. Turbul. 5 (4), 2004.